Neurodegenerative phenotypes in an A53T α-synuclein transgenic mouse model are independent of LRRK2

João Paulo L. Daher[1,2,6], Olga Pletnikova[3], Saskia Biskup[1,2,†], Alessandra Musso[7], Sandra Gellhaar[8], Dagmar Galter[8], Juan C. Troncoso[3], Michael K. Lee[9], Ted M. Dawson[1,2,4,10], Valina L. Dawson[1,2,4,5,10,*] and Darren J. Moore[7,*]

[1]NeuroRegeneration and Stem Cell Programs, Institute for Cell Engineering, [2]Department of Neurology, [3]Department of Pathology, [4]Department of Neuroscience and [5]Department of Physiology, Johns Hopkins University School of Medicine, Baltimore, MD 21205, USA, [6]Department of Pathology, School of Medicine, Fluminense Federal University, Niterói, Brazil [7]Brain Mind Institute, School of Life Sciences, Ecole Polytechnique Fédérale de Lausanne (EPFL), Lausanne 1015, Switzerland, [8]Department of Neuroscience, Karolinska Institute, Stockholm, Sweden, [9]Department of Neuroscience, Institute for Translational Neuroscience, University of Minnesota, Minneapolis, MN 55455, USA and [10]Adrienne Helis Malvin Medical Research Foundation, New Orleans, LA 70130-2685, USA

Mutations in the genes encoding LRRK2 and α-synuclein cause autosomal dominant forms of familial Parkinson's disease (PD). Fibrillar forms of α-synuclein are a major component of Lewy bodies, the intracytoplasmic proteinaceous inclusions that are a pathological hallmark of idiopathic and certain familial forms of PD. *LRRK2* mutations cause late-onset familial PD with a clinical, neurochemical and, for the most part, neuropathological phenotype that is indistinguishable from idiopathic PD. Importantly, α-synuclein-positive Lewy bodies are the most common pathology identified in the brains of PD subjects harboring *LRRK2* mutations. These observations may suggest that LRRK2 functions in a common pathway with α-synuclein to regulate its aggregation. To explore the potential pathophysiological interaction between LRRK2 and α-synuclein *in vivo*, we modulated LRRK2 expression in a well-established human A53T α-synuclein transgenic mouse model with transgene expression driven by the hindbrain-selective prion protein promoter. Deletion of LRRK2 or overexpression of human G2019S-LRRK2 has minimal impact on the lethal neurodegenerative phenotype that develops in A53T α-synuclein transgenic mice, including premature lethality, pre-symptomatic behavioral deficits and human α-synuclein or glial neuropathology. We also find that endogenous or human LRRK2 and A53T α-synuclein do not interact together to influence the number of nigrostriatal dopaminergic neurons. Taken together, our data suggest that α-synuclein-related pathology, which occurs predominantly in the hindbrain of this A53T α-synuclein mouse model, occurs largely independently from LRRK2 expression. These observations fail to provide support for a pathophysiological interaction of LRRK2 and α-synuclein *in vivo*, at least within neurons of the mouse hindbrain.

*To whom correspondence should be addressed at: Brain Mind Institute, Ecole Polytechnique Fédérale de Lausanne, AI 2150, Station 19, 1015 Lausanne, Switzerland. Tel: +41 216930971; Fax: +41 216930970; Email: darren.moore@epfl.ch (D.J.M.); NeuroRegeneration and Stem Cell Programs, Institute for Cell Engineering, Johns Hopkins University S.O.M., 733 North Broadway, BRB 731, Baltimore, MD 21205, USA. Tel: +1 4106143359; Fax: +1 4106149568; Email: vdawson@jhmi.edu (V.L.D.)
†Present address: Hertie Institute for Clinical Brain Research, University of Tübingen, 72076 Tübingen, Germany.

INTRODUCTION

Parkinson's disease (PD) typically occurs in a sporadic manner, although 5–10% of cases have a familial origin (1,2). Mutations in at least eight genes are known to cause familial forms of PD. Of these, mutations in the α-*synuclein* and *LRRK2* genes cause autosomal dominant forms of familial PD (1,2). Mutations in the *LRRK2* gene (PARK8, OMIM 609007) cause late-onset familial PD with a clinical and neurochemical phenotype that is indistinguishable from idiopathic PD (3–5). *LRRK2* mutations represent the most common known cause of PD (3). At least six missense mutations have been identified that segregate with disease in *LRRK2*-linked families, with the G2019S mutation representing the most common variant (3). The molecular basis of LRRK2-mediated neurodegeneration is poorly understood but may involve alterations in LRRK2-related signaling pathways or enzymatic activity (6–8).

Mutations in the α-*synuclein* gene (PARK1, OMIM 168601 and PARK4, OMIM 605543) represent a relatively rare cause of familial PD (1). Missense mutations (A30P, E46K and A53T) or gene multiplications cause disease in a small number of families (9–12). Common variation in the α-*synuclein* gene is associated with the risk of developing PD (13,14). α-Synuclein protein is the primary component of Lewy bodies, intracytoplasmic proteinaceous inclusions, which represent the hallmark neuropathology of sporadic and some familial forms of PD where they occur in surviving dopaminergic neurons of the substantia nigra (15). Mutations and increased gene dosage of α-synuclein promote its fibrillization and aggregation which is considered to underlie α-synuclein-mediated neurodegeneration (16).

The pathological interplay between LRRK2 and α-synuclein is poorly understood and whether they function in a common pathway, in parallel pathways or independently to mediate neurodegeneration in PD is not yet clear. In favor of a common pathway is the observation that the brains of PD subjects with *LRRK2* mutations predominantly exhibit α-synuclein-positive Lewy body pathology, suggesting that LRRK2 could lie upstream of α-synuclein to modulate its aggregation and toxicity (5,17,18). However, a formal proof of such a mechanism is currently lacking since LRRK2 transgenic mice and viral-based rodent models generally fail to develop α-synuclein-related pathology (19–25). Instead, certain LRRK2 rodent models can develop tau-related pathology which has also been reported in brains from certain PD subjects with *LRRK2* mutations albeit occurring less commonly than α-synuclein pathology (5,19,21,23,26). LRRK2 is also not a major component of Lewy bodies found in PD brains, suggesting that it is unlikely to be required for their formation (27–29).

In vitro studies have so far failed to demonstrate that α-synuclein is a direct substrate for the kinase activity of LRRK2 (30). A recent study has suggested that LRRK2 may function to inhibit the proteasome, thereby indirectly promoting the accumulation of α-synuclein and other proteasomal substrates (31). Moreover, LRRK2 was recently shown to regulate the progression of neuropathology induced by the expression of A53T α-synuclein selectively in mouse forebrain neurons (22). The pathologic interaction of α-synuclein and
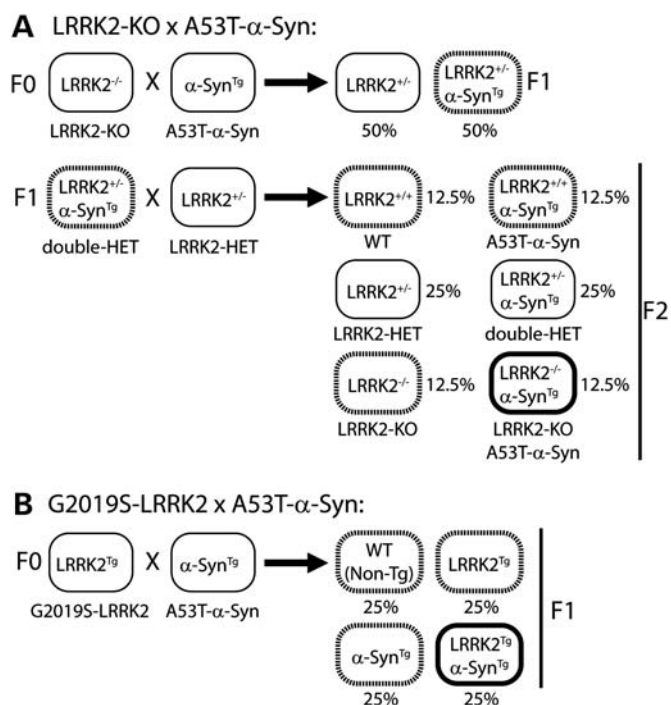

Figure 1. Breeding strategy to generate double mutant mice. (**A**) Strategy to generate A53T-α-Syn mice on an LRRK2 null background. F0, F1 and F2 represent each generation of crossbreeding. The expected frequency of each genotype is indicated as a percent. (**B**) Strategy to generate bigenic mice co-expressing A53T-α-Syn and G2019S-LRRK2.

LRRK2 in the regions of the nervous system that exhibit extensive pathology in PD is not known.

Here, we further explore the pathophysiological interplay between LRRK2 and α-synuclein *in vivo* by modulating LRRK2 expression in a well-established A53T α-synuclein transgenic mouse model under the control of the hindbrain-selective prion protein (PrP) promoter. We find that the overexpression of human G2019S-LRRK2 or the ablation of endogenous LRRK2 has minimal impact on the lethal neurodegenerative phenotype that occurs in A53T α-synuclein transgenic mice. Our data suggest that α-synuclein-related pathology in this mouse model occurs largely independently from LRRK2 expression, and further suggest that key differences may exist in the activity or function of LRRK2 between forebrain and hindbrain neurons.

RESULTS

Generation of A53T-α-Syn/LRRK2-knockout and A53T-α-Syn/G2019S-LRRK2 mice

To examine the potential interaction of α-synuclein and LRRK2 *in vivo*, mice were generated to overexpress human A53T mutant α-synuclein (A53T-α-Syn) either on an LRRK2 null background or with overexpression of human G2019S mutant LRRK2 (Fig. 1). We developed appropriate crossbreeding strategies of existing genetically modified mouse models. Mice in which both alleles of the *LRRK2* gene have been disrupted by targeted deletion of exon 40 [LRRK2-knockout (KO) mice] (32) were bred to A53T-α-Syn transgenic mice driven by the

mouse PrP promoter (33) in two successive breeding steps (Fig. 1A), as described previously (34). To minimize potential strain effects, LRRK2 heterozygous mice (LRRK2$^{+/-}$) were bred to double heterozygous mice (A53T-α-Syn^{Tg}/LRRK2$^{+/-}$) generated from the first round of breeding. We generated cohorts of age-matched littermates consisting of (i) wild-type (WT), (ii) LRRK2$^{-/-}$ (LRRK2^{KO}), (iii) A53T-α-Syn^{Tg} (Syn^{A53T}) and (iv) A53T-α-Syn^{Tg}/LRRK2$^{-/-}$ (Syn^{A53T}/LRRK2^{KO}) mice at expected Mendelian ratios for further analysis (Fig. 1A). Transgenic mice overexpressing human G2019S mutant LRRK2 driven by a hybrid CMV-enhanced platelet-derived growth factor-β chain (CMVe-PDGFβ) promoter (24) were bred to A53T-α-Syn transgenic mice. We crossed hemizygous G2019S-LRRK2 mice (G2019S-LRRK2^{Tg}) with hemizygous A53T-α-Syn mice to produce cohorts of age-matched littermates consisting of (i) WT, (ii) G2019S-LRRK2^{Tg} (LRRK2^{G2019S}), (iii) A53T-α-Syn^{Tg} (Syn^{A53T}) and (iv) G2019S-LRRK2^{Tg}/A53T-α-Syn^{Tg} (LRRK2^{G2019S}/Syn^{A53T}) genotypes at expected ratios (Fig. 1B).

Next, mRNA expression analysis was conducted in the individual mouse lines to assess the expression patterns of the A53T-α-Syn and G2019S-LRRK2 transgenes, as well as endogenous LRRK2 expression, in the brain by *in situ* hybridization with ^{33}P-labeled oligonucleotide probes (Fig. 2). Human A53T-α-Syn mRNA is expressed widely and abundantly throughout the brain of 7-month-old A53T-α-Syn transgenic mice compared with endogenous α-Syn mRNA using probes detecting total or mouse α-Syn (Fig. 2A). In these same mice, endogenous LRRK2 mRNA is also widely expressed but at comparatively lower levels and without differences between A53T-α-Syn transgenic and non-transgenic brains (Fig. 2A). Endogenous LRRK2 mRNA could be detected in the striatum, cerebral cortex, hippocampus, cerebellum and brainstem. Human G2019S-LRRK2 mRNA is also expressed widely throughout the brain of G2019S-LRRK2 transgenic mice, including the striatum, cerebral cortex, hippocampus, cerebellum and brainstem (Fig. 2B). The brain expression pattern and the level of human G2019S-LRRK2 or endogenous LRRK2 mRNA are similar at 9 and 12 months, demonstrating persistent LRRK2 expression with age (Fig. 2B). Importantly, human A53T-α-Syn and endogenous or human LRRK2 mRNAs are co-expressed throughout the brainstem, a region that displays a significant burden of α-Syn pathology in A53T-α-Syn transgenic mice (35). It has not been possible to co-localize α-Syn and LRRK2 mRNAs in brainstem neurons due to technical limitations, whereas at the protein level, detection of mouse or human LRRK2 in tissue sections has so far proven problematic with currently available antibodies (data not shown). Therefore, it is not possible to examine the co-localization of α-Syn and LRRK2 proteins in neuronal populations of the mouse brain using currently available reagents. Collectively, we demonstrate that human A53T-α-Syn, endogenous LRRK2 and human G2019S-LRRK2 are broadly expressed throughout the mouse brain where they are likely to be co-expressed in numerous anatomic regions and neuronal populations.
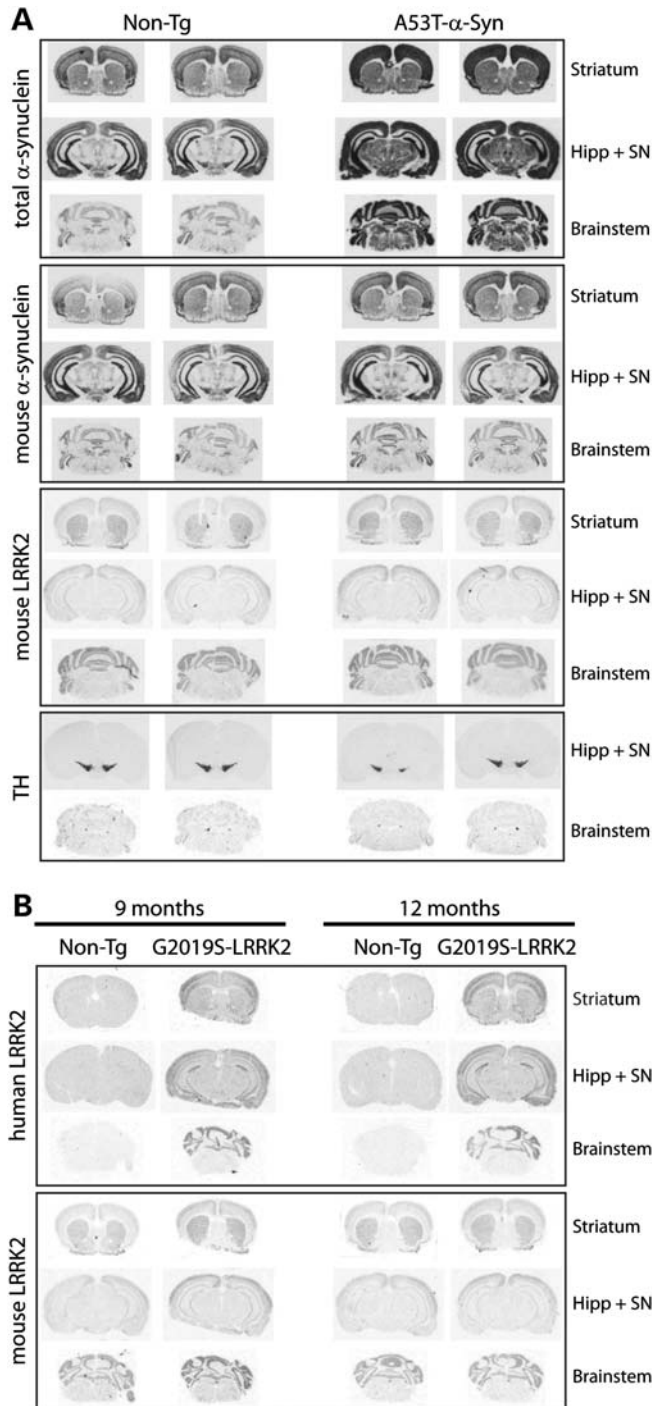

Figure 2. Localization of α-Syn and LRRK2 mRNA in the brain of transgenic mice. (**A**) *In situ* hybridization with ^{33}P-labeled antisense oligonucleotide probes specific to total (human + mouse) or mouse α-Syn, mouse LRRK2 or mouse TH. Autoradiographs indicate the localization of human and mouse α-Syn, or endogenous LRRK2 and TH mRNAs in tissue sections containing the striatum/cortex, hippocampus/substantia nigra (SN) and brainstem from 7-month-old human A53T-α-Syn transgenic mice and their non-transgenic (Non-Tg) littermate control mice. (**B**) Localization of human or mouse LRRK2 mRNA in brain sections from 9- or 12-month-old human G2019S-LRRK2 transgenic and their non-transgenic mice.
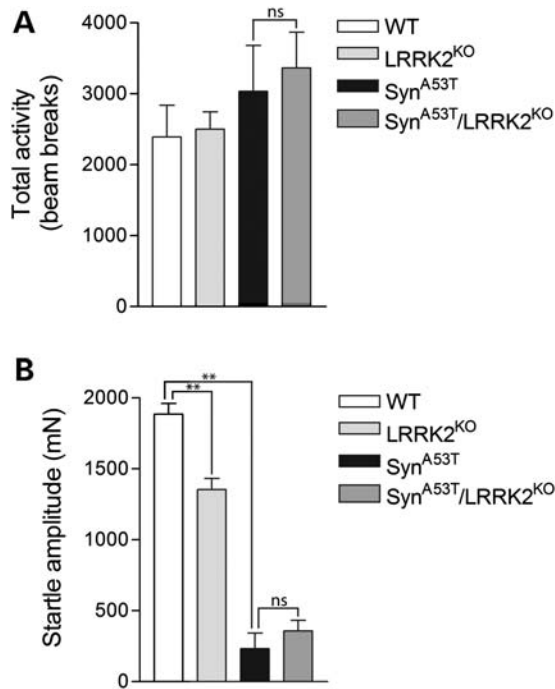
Figure 3. Behavioral deficits in A53T-α-Syn transgenic mice are not altered by the absence of LRRK. (**A**) In the open-field test, A53T-α-Syn mice and A53T-α-Syn/LRRK2-KO mice display a non-significant increase in locomotor activity compared with WT or LRRK2-KO mice at 6 months of age ($n = 4-7$ mice/genotype). Data indicate the total number of beam breaks during the first 15 min period expressed as mean $\pm$ SEM. (**B**) Analysis of acoustic startle reveals markedly reduced startle in A53T-α-Syn and A53T-α-Syn/LRRK2-KO mice, and a smaller reduction in the startle response in LRRK2-KO mice compared with WT control mice at 6 months of age ($n > 8$ mice/genotype). Data indicate startle amplitude in millinewtons (mN) expressed as mean $\pm$ SEM (**$P < 0.001$; n.s., non-significant).

Behavioral deficits in A53T-α-Syn transgenic mice are not altered by deletion of LRRK2

To begin to explore the impact of LRRK2 expression on the phenotype of A53T-α-Syn transgenic mice, we conducted behavioral analysis (Fig. 3). A53T-α-Syn mice normally exhibit pre-symptomatic hyperactivity prior to disease-onset (33,34). Accordingly, we focused on the effects of LRRK2 deletion on the locomotor activity of A53T-α-Syn transgenic mice in the open-field arena at 6 months of age. Both A53T-α-Syn and A53T-α-Syn/LRRK2-KO mice exhibit a non-significant increase in locomotor activity compared with their WT littermates, but do not differ significantly from each other (Fig. 3A). LRRK2-KO mice perform similarly to WT mice in the open field. A53T-α-Syn mice have previously been shown to exhibit an impaired acoustic startle response, a measure of sensorimotor gating in the brainstem (34). Therefore, we tested the acoustic startle response of A53T-α-Syn mice with or without LRRK2 deletion. Both A53T-α-Syn and A53T-α-Syn/LRRK2-KO mice display a dramatically impaired acoustic startle response compared with their WT littermates at 6 months of age (Fig. 3B). Importantly, however, the deficits exhibited by A53T-α-Syn and A53T-α-Syn/ LRRK2-KO mice are comparable and do not significantly differ from each other. Interestingly, LRRK2-KO mice exhibit a modest impairment of the acoustic startle response
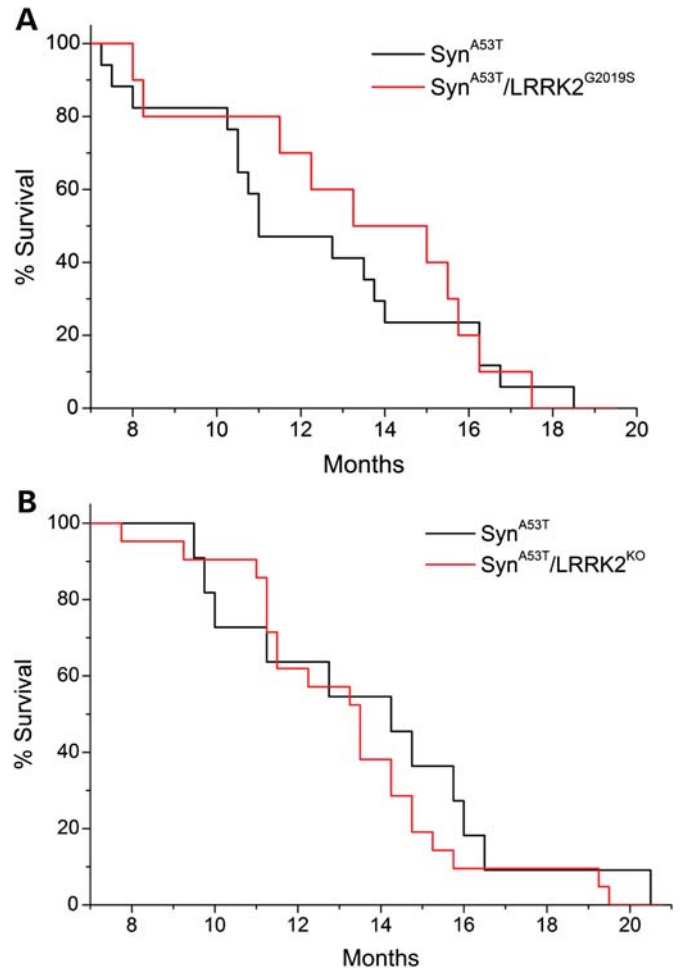

Figure 4. Progression of the lethal phenotype induced by expression of human A53T-α-Syn is independent of LRRK2. (**A**) The Kaplan–Meier survival curves of A53T-α-Syn and A53T-α-Syn/G2019S-LRRK2 mice were generated by monitoring cohorts of both genotypes (α-Syn^{A53T}, $n = 17$; α-Syn^{A53T}/LRRK2^{G2019S}, $n = 13$) until mice had to be euthanized due to the onset of terminal disease. (**B**) Survival curves of A53T-α-Syn (α-Syn^{A53T}, $n = 11$ mice) and A53T-α-Syn/LRRK2-KO (α-Syn^{A53T}/ LRRK2^{KO}, $n = 21$ mice) mice are also indicated.

compared with WT mice (Fig. 3B). Similar cohorts of A53T-α-Syn/G2019S-LRRK2 bigenic mice were not available for behavioral analysis. Collectively, our data demonstrate that A53T-α-Syn transgenic mice display mild hyperactivity and a markedly impaired acoustic startle response prior to disease-onset which is not modified by the deletion of LRRK2.

Premature lethality of A53T-α-Syn transgenic mice is independent of LRRK2

A53T-α-Syn transgenic mice display shortened lifespan owing to degeneration of brainstem and spinal cord neurons leading to limb paralysis, autonomic dysfunction and premature death (33–35). Accordingly, we assessed the impact of modulating LRRK2 expression on the survival of A53T-α-Syn mice (Fig. 4). A53T-α-Syn mice exhibit premature lethality ranging from 8 to 20 months of age. However, the survival of A53T-α-Syn/LRRK2-G2019S and A53T-α-Syn/LRRK2-KO
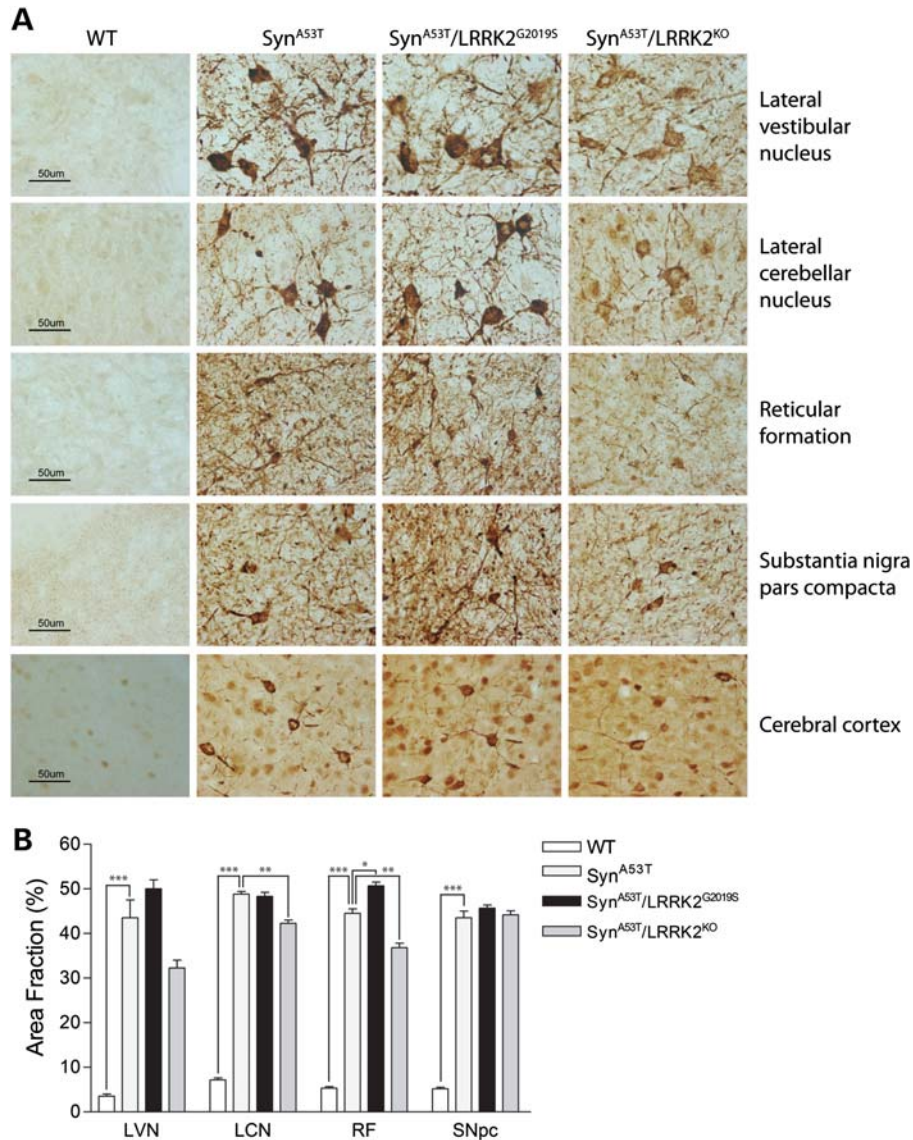
Figure 5. Abnormal accumulation of human α-Syn in the brainstem of A53T-α-Syn transgenic mice is modestly altered by modulating LRRK2 expression. (**A**) Representative images of phospho-Ser129-α-Syn immunoreactivity in the LVN, LCN, RF, SNpc and cerebral cortex from 13- to 14-month-old end-stage A53T-α-Syn, A53T-α-Syn/G2019S-LRRK2 or A53T-α-Syn/LRRK2-KO mice and their WT littermate controls. Human α-Syn pathology is absent from WT mice, whereas mice expressing A53T-α-Syn exhibit the abnormal accumulation of phospho-Ser129-α-Syn in neuronal cell bodies and processes. Scale bar: 50 μm. (**B**) Stereological assessment of phospho-Ser129-α-Syn immunoreactivity in distinct brain regions from each mouse genotype ($n = 3$ mice/genotype). Data represent the percent area fraction of immunoreactivity expressed as mean $\pm$ SEM (*$P < 0.05$, **$P < 0.01$ or ***$P < 0.001$).

double mutant mice does not significantly differ from that of single A53T-α-Syn transgenic mice (Fig. 4A and B). WT, G2019S-LRRK2 and LRRK2-KO mice typically exhibit normal survival up to 24 months of age (data not shown), as reported previously (24,32). Collectively, our data reveal that the premature death of A53T-α-Syn transgenic mice occurs independently of endogenous or pathogenic LRRK2 expression.

Modest alterations of neuropathology in A53T-α-Syn transgenic mice by LRRK2

To further explore the effects of LRRK2 expression on the neurodegenerative phenotype of A53T-α-Syn transgenic mice, we assessed the extent of neuropathology in end-stage

animals. Unbiased stereology was employed to quantify human α-Syn pathology and reactive gliosis in the brainstem and substantia nigra pars compacta (SNpc) of 13- to 14-month-old mice at the end-stage of disease (Fig. 5). Brainstem and nigral tissue were subjected to immunohistochemistry with an antibody to phospho-S129-α-Syn, a specific pathological form of human α-Syn. Human α-Syn pathology was evident throughout the brainstem, including the lateral vestibular nucleus (LVN), lateral cerebellar nucleus (LCN), reticular formation (RF), SNpc, cerebral cortex and striatum of A53T-α-Syn, A53T-α-Syn/LRRK2-G2019S and A53T-α-Syn/LRRK2-KO mice but was absent from WT mice (Fig. 5A). Quantitative stereological analysis demonstrates a modest yet significant reduction in human α-Syn pathology
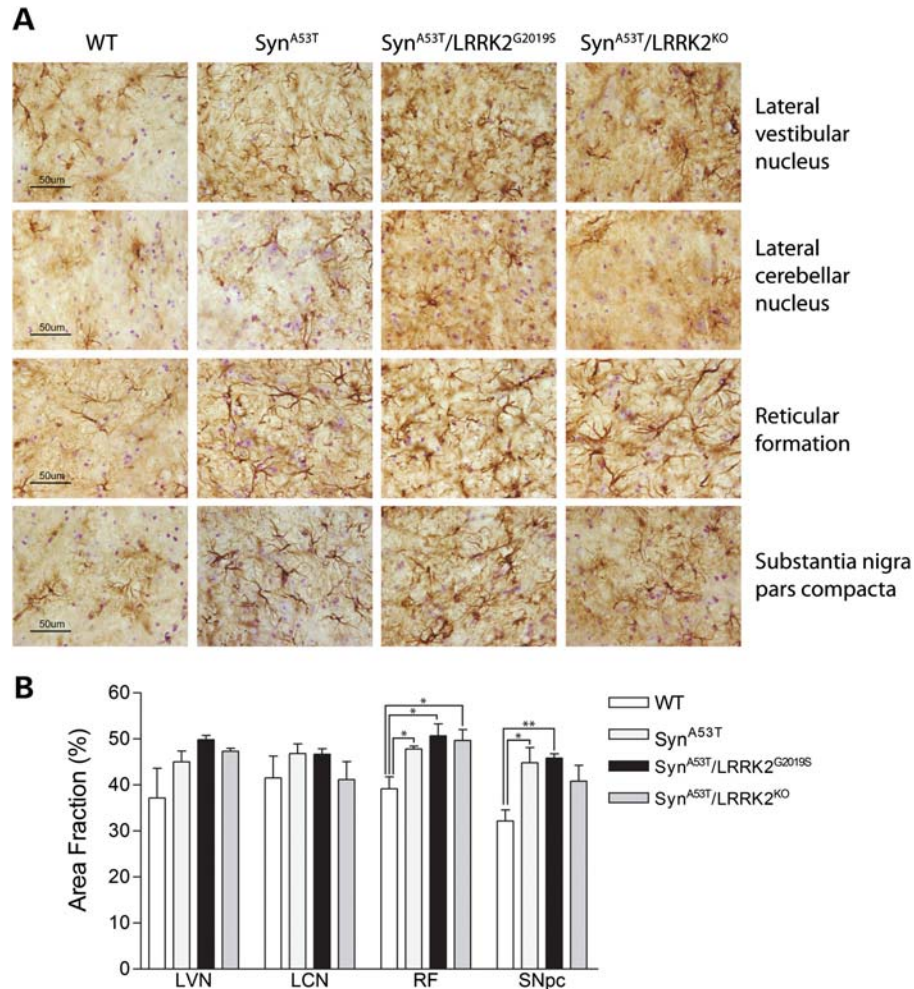
Figure 6. Astrocytic pathology in A53T-α-Syn transgenic mice is not affected by modulating LRRK2 expression. (**A**) Representative images of glial fibrillary acidic protein (GFAP) immunoreactivity in the LVN, LCN, RF and SNpc from 13- to 14-month-old end-stage A53T-α-Syn, A53T-α-Syn/G2019S-LRRK2 or A53T-α-Syn/LRRK2-KO mice and their WT littermate controls. A normal pattern of GFAP-positive astrocytic staining is observed in WT mice, whereas mice expressing human A53T-α-Syn reveal a marked astrocytic response in the RF and SNpc. Scale bar: 50 μm. (**B**) Stereological assessment of GFAP immunoreactivity in distinct brain regions from each mouse genotype ($n = 3$ mice/genotype). Data represent the percent area fraction of immunoreactivity expressed as mean $\pm$ SEM (*$P < 0.05$ or **$P < 0.01$).

in the LCN and RF, and a non-significant reduction ($P = 0.128$) in the LVN, of A53T-α-Syn/LRRK2-KO mice compared with single A53T-α-Syn mice (Fig. 5A and B). Human α-Syn pathology is modestly increased in the RF of A53T-α-Syn/LRRK2-G2019S mice compared with A53T-α-Syn mice (Fig. 5A and B). Human α-Syn pathology is not different in the SNpc between mouse genotypes (Fig. 5B). Our data demonstrate that LRRK2 deletion modestly and selectively reduces human α-Syn pathology in the brainstem of A53T-α-Syn transgenic mice, whereas G2019S-LRRK2 subtly enhances α-Syn pathology.

We also explored the effects of LRRK2 expression on the level of astroglial and microglial pathology in the brainstem and SNpc of A53T-α-Syn transgenic mice (34). Immunoreactivity for the astrocytic marker, glial fibrillary acidic protein (GFAP), was significantly increased in the RF and SNpc of A53T-α-Syn mice compared with WT mice, whereas there is a non-significant increase in the LVN and LCN (Fig. 6A and B). GFAP pathology does not, however, provide a sensitive

marker to discriminate between A53T-α-Syn, A53T-α-Syn/LRRK2-G2019S and A53T-α-Syn/LRRK2-KO mice. Similarly, A53T-α-Syn mice exhibit a non-significant increase in immunoreactivity for the microglial marker, Iba1, in the RF but not in the LCN compared with WT mice (Fig. 7A and B). However, Iba1 pathology in A53T-α-Syn/LRRK2-G2019S and A53T-α-Syn/LRRK2-KO mice does not significantly differ from A53T-α-Syn mice. Our data suggest that reactive gliosis evident in the brainstem and substantia nigra of A53T-α-Syn mice occurs independent of LRRK2 expression.

Modulation of LRRK2 expression in A53T-α-Syn transgenic mice fails to influence the number of nigrostriatal dopaminergic neurons

The expression of G2019S-LRRK2 in transgenic mice has been shown to induce the age-dependent degeneration of nigrostriatal dopaminergic neurons with neuronal loss occurring at ∼20 months of age (24). We also notice that
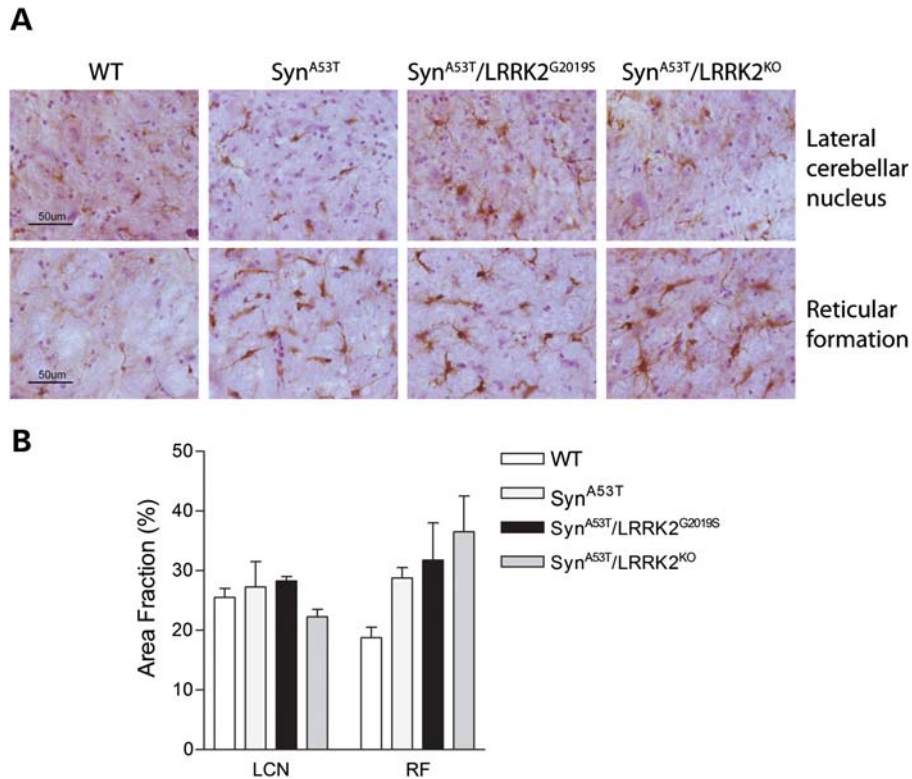
Figure 7. Microglial pathology in A53T-α-Syn transgenic mice is not affected by modulating LRRK2 expression. (**A**) Representative images of Iba1 immunoreactivity in the LCN and RF from 13- to 14-month-old end-stage A53T-α-Syn, A53T-α-Syn/G2019S-LRRK2 or A53T-α-Syn/LRRK2-KO mice and their WT littermate controls. A normal pattern of Iba1-positive microglial staining is observed in WT mice, whereas mice expressing human A53T-α-Syn reveal a marked microglial response in the RF but not the LCN. Scale bar: 50 μm. (**B**) Stereological assessment of Iba1 immunoreactivity in the LCN and RF from each mouse genotype ($n = 3$ mice/genotype). Data represent the percent area fraction of immunoreactivity expressed as mean ± SEM. There are no statistical differences between mouse genotypes ($P > 0.05$).

A53T-α-Syn transgenic mice display a substantial burden of α-Syn pathology in neurons of the SNpc (Fig. 5). To evaluate a potential pathological interaction of A53T-α-Syn and LRRK2 in the nigrostriatal dopaminergic pathway, we assessed the dopaminergic neuronal number in the substantia nigra of end-stage animals (Fig. 8). We conducted unbiased stereological assessments of tyrosine hydroxylase (TH)-positive and Nissl-positive dopaminergic neurons in the SNpc to evaluate neuronal loss. In 13- to 14-month-old end-stage mice, we do not observe dopaminergic neuronal loss in A53T-α-Syn or G2019S-LRRK2 transgenic mice, or LRRK2-KO mice, compared with WT littermate mice (Fig. 8A–D). The co-expression of A53T-α-Syn and G2019S-LRRK2 in bigenic mice does not influence the nigral dopaminergic neuronal number compared with single transgenic or WT mice (Fig. 8A and B). Furthermore, A53T-α-Syn/LRRK2-KO mice display a normal complement of dopaminergic neurons compared with control littermates (Fig. 8C and D). These data suggest that A53T-α-Syn and LRRK2 do not interact together to modulate the number of nigrostriatal dopaminergic neurons.

DISCUSSION

In this study, we report the impact of modulating LRRK2 expression on the lethal neurodegenerative phenotype of A53T-α-Syn transgenic mice. Human α-Syn and endogenous or human LRRK2 are broadly co-expressed throughout the mouse brain including within forebrain, midbrain and hindbrain regions. The overexpression of human G2019S-LRRK2 or LRRK2 deletion fails to influence the premature lethality of A53T-α-Syn mice, whereas LRRK2 deletion has no impact on pre-symptomatic behavioral deficits in these mice. LRRK2 deletion modestly reduces human α-Syn pathology in certain brainstem nuclei of A53T-α-Syn mice, whereas expression of G2019S-LRRK2 subtly enhances brainstem α-Syn pathology. However, altering LRRK2 expression fails to modulate glial pathology in the brainstem and substantia nigra of A53T-α-Syn mice. Finally, human A53T-α-Syn and endogenous or human LRRK2 do not pathologically interact together to regulate the number of nigrostriatal dopaminergic neurons. Taken together, our data suggest that neurodegenerative phenotypes that develop in PrP promoter-driven A53T-α-Syn transgenic mice occur largely independently from LRRK2 expression.

LRRK2 expression modestly regulates human α-Syn pathology in select brainstem nuclei of A53T-α-Syn mice. LRRK2 deletion reduced α-Syn pathology in the LCN and RF, whereas G2019S-LRRK2 enhanced pathology in the RF. The effects on α-Syn pathology are rather subtle and fail to occur in additional brainstem nuclei or within the SNpc, despite substantial α-Syn pathology in these regions. Furthermore, although glial pathology is evident in A53T-α-Syn
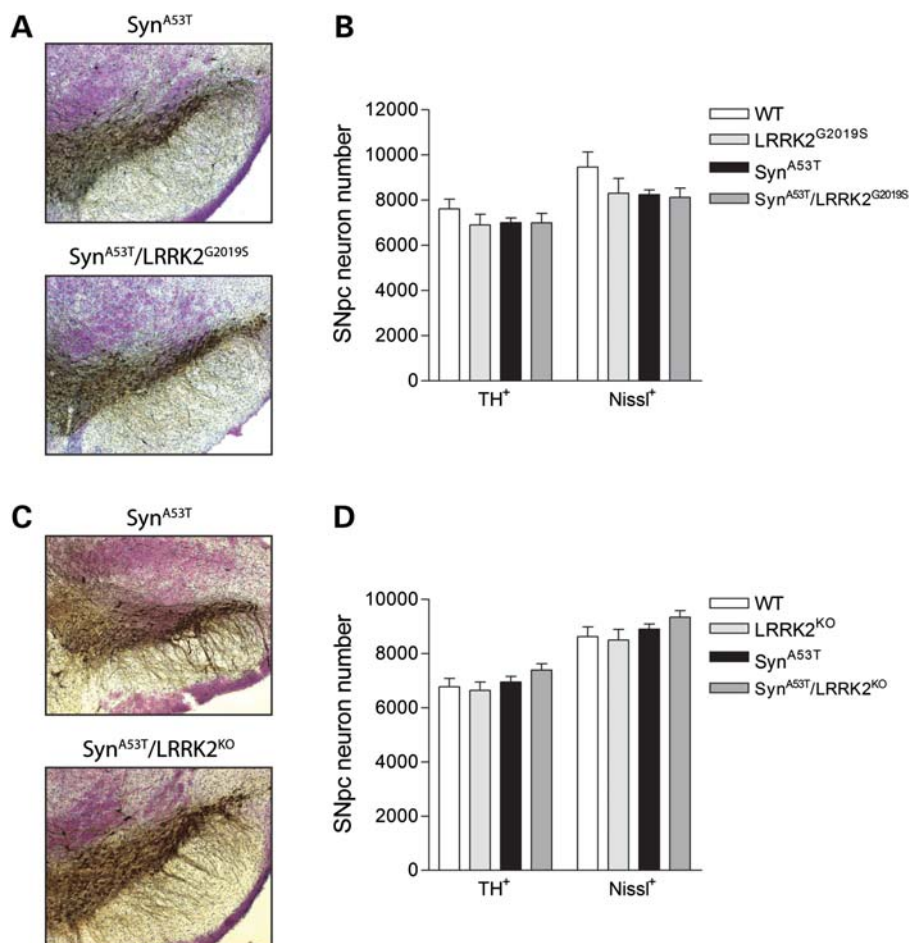
Figure 8. A53T-α-Syn and LRRK2 do not interact to influence the number of nigrostriatal dopaminergic neurons in mice. (**A** and **C**) Representative images of TH-positive neurons in the SNpc of 13- to 14-month-old end-stage A53T-α-Syn, A53T-α-Syn/G2019S-LRRK2 and A53T-α-Syn/LRRK2-KO mice. (**B** and **D**) Stereological assessment of the number of TH-positive and Nissl-positive dopaminergic neurons in the SNpc for each mouse genotype generated by crossbreeding of (B) A53T-α-Syn and LRRK2-G2019S transgenic mice ($n = 3-6$ mice/genotype) or (D) A53T-α-Syn and LRRK2-KO mice ($n = 4$ mice/genotype). Data represent the number of TH+ or Nissl+ SNpc neurons expressed as mean $\pm$ SEM. There are no statistical differences between mouse genotypes ($P > 0.05$).

mice, there is no significant influence of LRRK2 expression on the extent of reactive gliosis. These observations may suggest that α-Syn pathology occurs largely independently of LRRK2 expression in this A53T-α-Syn mouse model or that LRRK2 is located downstream of α-Syn pathology where it would be expected to have minimal impact on the development of pathology. However, this potential latter mechanism would not be consistent with the occurrence of α-Syn pathology in PD brains harboring *LRRK2* mutations (5,17,18), where LRRK2 clearly lies upstream of α-Syn aggregation. Alternatively, our findings could potentially be explained by a lack of co-expression of human α-Syn and LRRK2 in neuronal populations that develop pathology in A53T-α-Syn mice. Current antibodies are not useful for reliably assessing the localization of LRRK2 in the mouse brain. Instead, *in situ* hybridization analysis of endogenous and human LRRK2 mRNA revealed a broad distribution throughout the mouse brain including the brainstem, whereas previous studies have shown that endogenous LRRK2 or human G2019S-LRRK2 are expressed at low levels in the substantia nigra (24,36,37). Based on these expression data, it would be expected that endogenous and/or human LRRK2 would co-localize with human α-Syn

in a substantial number of neuronal populations in the brainstem and elsewhere throughout the brain.

A recent study using inducible transgenic mice demonstrated that the specific co-expression of human G2019S-LRRK2 and human A53T-α-Syn in CamKIIα-positive neurons of the forebrain dramatically enhanced α-Syn-mediated neuropathology in the striatum and cortex, whereas ablation of LRRK2 reduced this neuropathology (22). However, the functional significance of this altered α-Syn pathology was not assessed at the level of motor behavior or survival. In the PrP promoter-driven A53T-α-Syn mice, hyperactivity and impaired acoustic startle that occur prior to disease-onset were unaffected by the deletion of LRRK2. Furthermore, the premature lethality of A53T-α-Syn mice owing to the progressive degeneration of neuronal populations located in the brainstem and spinal cord was not altered by modulating LRRK2 expression. Therefore, at least in the hindbrain where the majority of α-Syn pathology develops in the PrP–A53T-α-Syn mice (33–35), LRRK2 expression appears to play an insignificant role at a functional level while subtly altering α-Syn pathology in discrete brainstem nuclei. These observations may indicate that LRRK2 activity or

function may be more physiologically important in forebrain regions such as the striatum and cortex where LRRK2 is normally expressed at highest levels, compared with midbrain and hindbrain regions where LRRK2 expression is less abundant (28,36–40). The mechanism by which LRRK2 regulates human α-Syn pathology in A53T-α-Syn transgenic mice in this and previous studies (22) is unclear at present. LRRK2 could potentially impair microtubule dynamics, Golgi complex integrity and/or the ubiquitin–proteasomal pathway to indirectly regulate α-Syn accumulation and aggregation (22,31). Whether LRRK2 enzymatic activity is required for modulating α-Syn neuropathology *in vivo* is not yet clear but would have important implications for the development of disease-modifying therapies. The efficacy of LRRK2 kinase inhibitors for attenuating neurodegenerative phenotypes in A53T-α-Syn rodent models is worthwhile evaluating in future studies.

Collectively, our study demonstrates that LRRK2 expression plays an insignificant role in the development of neurodegenerative phenotypes occurring in A53T-α-Syn transgenic mice under the control of the hindbrain-selective PrP promoter. Future studies will aim to further clarify the pathophysiological interaction of α-Syn and LRRK2 in the mammalian brain and whether this interaction is of greater significance to distinct neuronal populations such as those located in the striatum and cortex where LRRK2 is normally most abundant. It will also be important to oppositely explore the role of α-Syn expression in LRRK2-mediated neurodegeneration in animal models which would perhaps best recapitulate the molecular pathway occurring in PD subjects with *LRRK2* mutations and α-Syn-positive Lewy body pathology.

MATERIALS AND METHODS

Animals

Mice were housed and treated in strict accordance with the NIH Guide for the Care and Use of Laboratory Animals. All animal procedures were approved by the Institutional Animal Care and Use Committees of the Johns Hopkins Medical Institutions (Animal Welfare Assurance No. A3272-01) or were conducted in accordance with the Swiss legislation (Canton de Vaud, Animal Authorization No. 2293) and the European Union directive (2010/63/EU) for the protection of animals used for scientific purposes. Mice were maintained in a pathogen-free barrier facility and exposed to a 12 h light/dark cycle with food and water provided *ad libitum*.

Generation of double mutant mice

Transgenic mice with overexpression of human A53T-α-Syn under the control of the mouse PrP promoter (line G2-3) were described previously (33–35) and have been maintained on a C57BL/6J background following at least 10 generations of backcrossing. LRRK2-KO mice with deletion of partial exon 39 and complete exon 40 were reported previously (32), and subsequently maintained on a C57BL76J background. Transgenic mice with overexpression of human G2019S-LRRK2 under the control of a CMVe-PDGFβ promoter (line 340) were reported previously (24) and maintained

on a C57BL76J background. Double mutant mice overexpressing A53T-α-Syn in the absence of LRRK2 (A53T-α-Syn/LRRK2-KO) and appropriate littermate controls were generated in two successive crossbreeding steps as described previously (34). Briefly, homozygous LRRK2-KO mice were crossed with hemizygous A53T-α-Syn mice to generate double mutant mice (A53T-α-Syn[Tg]/LRRK2^{+/−}). These progeny were crossed with heterozygous LRRK2^{+/−} mice to produce all four genotypes for analysis. Bigenic mice were generated by crossing hemizygous A53T-α-Syn and G2019S-LRRK2 transgenic mice in a single crossbreeding step. Mice were identified by genomic PCR with specific primer pairs: G2019S-LRRK2 transgenic mice (CMVe-F1, 5′-ATTACCATGGTTCGAGGTGA-3′ and CMVe-R1, 5′-CAAGTGTCTGCAGGAAGGTT-3′ producing a ∼170 bp DNA fragment) or PrP-A53T-α-Syn mice (hSYN-S, 5′-TTCATGAAAGGACTTTCAAAGGC-3′ and PrP-AS, 5′-GTGGATACCCCCTCCCCCAGCCTAGACC-3′ producing a ∼450 bp DNA fragment) together with mouse glyceraldehyde 3-phosphate dehydrogenase (GAPDH) primers (GAPDH-F1, 5′-TGTTTGTGATGGGTGTGAAC-3′ and GAPDH-R1, 5′-TACTTGGCAGGTTTCTCCAG-3′ producing a ∼380 bp DNA fragment) and LRRK2-KO mice (forward, 5′-CCCAGGGCTGAGAACGATTAAGTC-3′ and reverse, 5′-CTGGAGTGGACTCAGGGTTACAGC-3′ producing a 590 bp DNA fragment from the WT LRRK2 allele, and primer pair forward, 5′-GGCCTACCCGCTTCCATTGCTCAGCGG-3′ and reverse, 5′-CCGAACAAACGACCCAACACCCGTGCG-3′ producing a 328 bp DNA fragment from mutant LRRK2 allele).

Immunohistochemistry and histology

Immunohistochemistry was performed after intracardiac perfusion of mice with 1× phosphate-buffered saline and 4% paraformaldehyde (PFA). Brains were then removed, fixed overnight in 4% PFA and cryopreserved in 30% sucrose for 48 h. Coronal sections (40 μm) from 13- to 14-month-old animals were prepared and processed for various pathologic markers as described previously (24,34). Tissue sections were quenched for endogenous peroxidase activity, permeabilized and incubated with rabbit anti-phospho-Ser129-α-synuclein (Wako Chemicals, Richmond, VA, USA), mouse anti-GFAP (Sigma-Aldrich, St Louis, MO, USA) or rabbit anti-Iba1 (Wako Chemicals) antibodies. Sections were processed with biotinylated anti-rabbit or anti-mouse IgG (Jackson ImmunoResearch, West Grove, PA, USA) and avidin–biotin complex coupled to horseradish peroxidase (Vectastain ABC; Vector Laboratories, Burlingame, CA, USA) and visualized with 3,3′-diaminobenzidine (Sigma-Aldrich). Sections were mounted, air dried, counterstained with cresyl violet, dehydrated and coverslipped.

Stereological measurements of nigrostriatal dopaminergic cells

Coronal midbrain sections (40 μm) from 13- to 14-month-old end-stage symptomatic mice and their aged-matched control littermates were processed for immunohistochemistry with rabbit anti-TH antibody (Novus Biologicals, Littleton, CO,

USA) and Nissl counterstain, as described previously (24,41). Unbiased stereological methodology was employed to count TH+ and Nissl+ neurons in the left and right SNpc region of every fourth section throughout the ventral midbrain, as described previously (24,41,42). Stereological counts were obtained using a computer-assisted image analysis system consisting of an Axiophot 2 photomicroscope (Carl Zeiss Inc., Thornwood, NY, USA) equipped with a computer-controlled motorized stage (Ludl Electronics, Hawthorne, NY, USA), a Hitachi HV C20 video camera, and interfaced with a StereoInvestigator system (MicroBrightField Inc., Williston, VT, USA) with optical fractionator probe. We used a counting frame of 40×40 μm, a 1 μm guard, a sampling grid of 100×100 μm and a dissector height of 8 μm. For Nissl counting, a cell was defined as a bright blue-stained neuronal perikarya with a nucleolus. Nissl-positive counts were restricted to Nissl+/TH+ neurons along with large Nissl+ neurons with dopaminergic-like morphology, which contain little or no TH immunostaining. Counts were performed by investigators blinded to the genotype of each animal.

Stereological measurements of immunoreactive areas

Area fraction analysis was performed as described previously (43). Coronal brain sections (40 μm) from matched anatomical regions for each mouse genotype ($n = 3$ brains per genotype, 1 section per region) were selected for each antibody (pSer129-α-synuclein, GFAP or Iba1). After immunostaining, each section was first microscopically assessed at low magnification ($\times 5$ objective) to identify regions with the highest level of phospho-Ser129-α-synuclein, GFAP or Iba1 immunoreactivity. A StereoInvestigator system (MicroBrightField Inc.) and a $\times 5$ objective were used to mark the contours encompassing the right and left SNpc, LCN, LVN and RF. Immunoreactivity within each area (right and left sides) was measured using a $\times 40$ objective and the area-fraction fractionator probe (sampling grid size: SNpc, 300×300 μm; LCN, 175×150 μm; LVN, 150×100 μm; RF, 200×100 μm). At each sampling site, a counting grid (SNpc, 300×300 μm; LCN, 175×150 μm; LVN, 150×100 μm; RF, 200×100 μm) was superimposed consisting of markers equally spaced from one another at a distance of 15 μm. Markers that co-localized with immunoreactivity were labeled as positive, whereas remaining markers were labeled as negative. The area fraction was calculated as the number of positive markers divided by the total number of markers superimposed on the counting frame. Stereological assessments were performed by investigators blinded to the genotype of each animal.

In situ hybridization

Fresh-frozen coronal sections from A53T-α-Syn (7 months-old) or G2019S-LRRK2 (9 or 12 months-old) transgenic mice, and their age-matched non-transgenic littermate controls were subjected to *in situ* hybridization as previously described (24,44) using ^{33}P-labeled oligonucleotide probes complementary to mouse/human α-synuclein (nt 522–571; NM_007308.2), mouse α-synuclein (nt 738–787; NM_

001042451.1), human LRRK2 (nt 4436–4483; NM_198578.3), mouse LRRK2 (nt 6036–6085; NM_025730.2) or mouse TH (nt 197–248; NM_009377.1). Messenger RNA signals were revealed by exposure of slides to autoradiographic film or were dipped in photographic emulsion (NB2, Kodak) for microscopy analysis.

Behavioral analysis

Behavioral analysis of A53T-α-Syn/LRRK2-KO mice and their littermate controls at 6 months of age were conducted as described previously (24,34). 'Open-field test': novelty-induced locomotor activity in the open-field quadrant was assessed over a 60 min period using a Cage Rack Flex-Field Photobeam Activity System (San Diego Instruments, San Diego, CA, USA) which provides horizontal and vertical grids of 16×16 infrared beams. The total number of beam breaks in both horizontal and vertical planes was recorded during the test. Activity during the first 15 min period was used for analysis. 'Acoustic startle response': for acoustic startle, mice were assessed for the maximal amplitude of the acoustic startle response in an SR-LAB Startle Reflex system (San Diego Instruments). Mice were habituated by 5 min of background noise and then exposed to a series of acoustic stimuli (40 ms duration) ranging from 75 to 120 dB, including two 0 dB baseline measurements, occurring in a pseudorandom order. The interval between each stimulus was 15 s, and the series of stimuli were repeated six times. The maximal amplitude of each motor response was determined. The average value of six repeats for the 120 dB stimulus intensity was calculated and used for statistical analysis of mouse genotypes.

Statistical analysis

Data were expressed as mean $\pm$ SEM. Statistical analysis was performed by one-way ANOVA with Newman–Keuls *post hoc* test. A value of $P < 0.05$ was considered significant.

engagement in the continuous active conduct of medical research in conjunction with The Johns Hopkins Hospital and the Johns Hopkins University School of Medicine and the Foundation's Parkinson's Disease Program No. M-1.

REFERENCES

1. Gasser, T. (2009) Mendelian forms of Parkinson's disease. *Biochim. Biophys. Acta*, **1792**, 587–596.
2. Hardy, J., Lewis, P., Revesz, T., Lees, A. and Paisan-Ruiz, C. (2009) The genetics of Parkinson's syndromes: a critical review. *Curr. Opin. Genet. Dev.*, **19**, 254–265.
3. Healy, D.G., Falchi, M., O'Sullivan, S.S., Bonifati, V., Durr, A., Bressman, S., Brice, A., Aasly, J., Zabetian, C.P., Goldwurm, S. *et al.* (2008) Phenotype, genotype, and worldwide genetic penetrance of LRRK2-associated Parkinson's disease: a case–control study. *Lancet Neurol.*, **7**, 583–590.
4. Paisan-Ruiz, C., Jain, S., Evans, E.W., Gilks, W.P., Simon, J., van der Brug, M., Lopez de Munain, A., Aparicio, S., Gil, A.M., Khan, N. *et al.* (2004) Cloning of the gene containing mutations that cause PARK8-linked Parkinson's disease. *Neuron*, **44**, 595–600.
5. Zimprich, A., Biskup, S., Leitner, P., Lichtner, P., Farrer, M., Lincoln, S., Kachergus, J., Hulihan, M., Uitti, R.J., Calne, D.B. *et al.* (2004) Mutations in LRRK2 cause autosomal-dominant parkinsonism with pleomorphic pathology. *Neuron*, **44**, 601–607.
6. Biskup, S. and West, A.B. (2009) Zeroing in on LRRK2-linked pathogenic mechanisms in Parkinson's disease. *Biochim. Biophys. Acta*, **1792**, 625–633.
7. Cookson, M.R. (2010) The role of leucine-rich repeat kinase 2 (LRRK2) in Parkinson's disease. *Nat. Rev. Neurosci.*, **11**, 791–797.
8. Moore, D.J. (2008) The biology and pathobiology of LRRK2: implications for Parkinson's disease. *Parkinsonism Relat. Disord.*, **14** (Suppl. 2), S92–S98.
9. Polymeropoulos, M.H., Lavedan, C., Leroy, E., Ide, S.E., Dehejia, A., Dutra, A., Pike, B., Root, H., Rubenstein, J., Boyer, R. *et al.* (1997) Mutation in the alpha-synuclein gene identified in families with Parkinson's disease. *Science*, **276**, 2045–2047.
10. Kruger, R., Kuhn, W., Muller, T., Woitalla, D., Graeber, M., Kosel, S., Przuntek, H., Epplen, J.T., Schols, L. and Riess, O. (1998) Ala30Pro mutation in the gene encoding alpha-synuclein in Parkinson's disease. *Nat. Genet.*, **18**, 106–108.
11. Zarranz, J.J., Alegre, J., Gomez-Esteban, J.C., Lezcano, E., Ros, R., Ampuero, I., Vidal, L., Hoenicka, J., Rodriguez, O., Atares, B. *et al.* (2004) The new mutation, E46K, of alpha-synuclein causes Parkinson and Lewy body dementia. *Ann. Neurol.*, **55**, 164–173.
12. Singleton, A.B., Farrer, M., Johnson, J., Singleton, A., Hague, S., Kachergus, J., Hulihan, M., Peuralinna, T., Dutra, A., Nussbaum, R. *et al.* (2003) Alpha-Synuclein locus triplication causes Parkinson's disease. *Science*, **302**, 841.
13. Simon-Sanchez, J., Schulte, C., Bras, J.M., Sharma, M., Gibbs, J.R., Berg, D., Paisan-Ruiz, C., Lichtner, P., Scholz, S.W., Hernandez, D.G. *et al.* (2009) Genome-wide association study reveals genetic risk underlying Parkinson's disease. *Nat. Genet.*, **41**, 1308–1312.
14. Satake, W., Nakabayashi, Y., Mizuta, I., Hirota, Y., Ito, C., Kubo, M., Kawaguchi, T., Tsunoda, T., Watanabe, M., Takeda, A. *et al.* (2009) Genome-wide association study identifies common variants at four loci as genetic risk factors for Parkinson's disease. *Nat. Genet.*, **41**, 1303–1307.
15. Spillantini, M.G., Schmidt, M.L., Lee, V.M., Trojanowski, J.Q., Jakes, R. and Goedert, M. (1997) Alpha-synuclein in Lewy bodies. *Nature*, **388**, 839–840.
16. Waxman, E.A. and Giasson, B.I. (2009) Molecular mechanisms of alpha-synuclein neurodegeneration. *Biochim. Biophys. Acta*, **1792**, 616–624.
17. Giasson, B.I., Covy, J.P., Bonini, N.M., Hurtig, H.I., Farrer, M.J., Trojanowski, J.Q. and Van Deerlin, V.M. (2006) Biochemical and pathological characterization of Lrrk2. *Ann. Neurol.*, **59**, 315–322.
18. Ross, O.A., Toft, M., Whittle, A.J., Johnson, J.L., Papapetropoulos, S., Mash, D.C., Litvan, I., Gordon, M.F., Wszolek, Z.K., Farrer, M.J. *et al.* (2006) Lrrk2 and Lewy body disease. *Ann. Neurol.*, **59**, 388–393.
19. Dusonchet, J., Kochubey, O., Stafa, K., Young, S.M. Jr., Zufferey, R., Moore, D.J., Schneider, B.L. and Aebischer, P. (2011) A rat model of progressive nigral neurodegeneration induced by the Parkinson's disease-associated G2019S mutation in LRRK2. *J. Neurosci.*, **31**, 907–912.
20. Li, X., Patel, J.C., Wang, J., Avshalumov, M.V., Nicholson, C., Buxbaum, J.D., Elder, G.A., Rice, M.E. and Yue, Z. (2010) Enhanced striatal dopamine transmission and motor performance with LRRK2 overexpression in mice is eliminated by familial Parkinson's disease mutation G2019S. *J. Neurosci.*, **30**, 1788–1797.
21. Li, Y., Liu, W., Oo, T.F., Wang, L., Tang, Y., Jackson-Lewis, V., Zhou, C., Geghman, K., Bogdanov, M., Przedborski, S. *et al.* (2009) Mutant LRRK2(R1441G) BAC transgenic mice recapitulate cardinal features of Parkinson's disease. *Nat. Neurosci.*, **12**, 826–828.
22. Lin, X., Parisiadou, L., Gu, X.L., Wang, L., Shim, H., Sun, L., Xie, C., Long, C.X., Yang, W.J., Ding, J. *et al.* (2009) Leucine-rich repeat kinase 2 regulates the progression of neuropathology induced by Parkinson's-disease-related mutant alpha-synuclein. *Neuron*, **64**, 807–827.
23. Melrose, H.L., Daechsel, J.C., Behrouz, B., Lincoln, S.J., Yue, M., Hinkle, K.M., Kent, C.B., Korvatska, E., Taylor, J.P., Witten, L. *et al.* (2010) Impaired dopaminergic neurotransmission and microtubule-associated protein tau alterations in human LRRK2 transgenic mice. *Neurobiol. Dis.*, **40**, 503–517.
24. Ramonet, D., Daher, J.P., Lin, B.M., Stafa, K., Kim, J., Banerjee, R., Westerlund, M., Pletnikova, O., Glauser, L., Yang, L. *et al.* (2011) Dopaminergic neuronal loss, reduced neurite complexity and autophagic abnormalities in transgenic mice expressing G2019S mutant LRRK2. *PLoS One*, **6**, e18568.
25. Tong, Y., Pisani, A., Martella, G., Karouani, M., Yamaguchi, H., Pothos, E.N. and Shen, J. (2009) R1441C mutation in LRRK2 impairs dopaminergic neurotransmission in mice. *Proc. Natl Acad. Sci. USA*, **106**, 14622–14627.
26. Rajput, A., Dickson, D.W., Robinson, C.A., Ross, O.A., Dachsel, J.C., Lincoln, S.J., Cobb, S.A., Rajput, M.L. and Farrer, M.J. (2006) Parkinsonism, Lrrk2 G2019S, and tau neuropathology. *Neurology*, **67**, 1506–1508.
27. Greggio, E., Jain, S., Kingsbury, A., Bandopadhyay, R., Lewis, P., Kaganovich, A., van der Brug, M.P., Beilina, A., Blackinton, J., Thomas, K.J. *et al.* (2006) Kinase activity is required for the toxic effects of mutant LRRK2/dardarin. *Neurobiol. Dis.*, **23**, 329–341.
28. Higashi, S., Biskup, S., West, A.B., Trinkaus, D., Dawson, V.L., Faull, R.L., Waldvogel, H.J., Arai, H., Dawson, T.M., Moore, D.J. *et al.* (2007) Localization of Parkinson's disease-associated LRRK2 in normal and pathological human brain. *Brain Res.*, **1155**, 208–219.
29. Higashi, S., Moore, D.J., Yamamoto, R., Minegishi, M., Sato, K., Togo, T., Katsuse, O., Uchikado, H., Furukawa, Y., Hino, H. *et al.* (2009) Abnormal localization of leucine-rich repeat kinase 2 to the endosomal–lysosomal compartment in lewy body disease. *J. Neuropathol. Exp. Neurol.*, **68**, 994–1005.
30. West, A.B., Moore, D.J., Biskup, S., Bugayenko, A., Smith, W.W., Ross, C.A., Dawson, V.L. and Dawson, T.M. (2005) Parkinson's disease-associated mutations in leucine-rich repeat kinase 2 augment kinase activity. *Proc. Natl Acad. Sci. USA*, **102**, 16842–16847.
31. Lichtenberg, M., Mansilla, A., Zecchini, V.R., Fleming, A. and Rubinsztein, D.C. (2011) The Parkinson's disease protein LRRK2 impairs proteasome substrate clearance without affecting proteasome catalytic activity. *Cell Death Dis.*, **2**, e196.
32. Andres-Mateos, E., Mejias, R., Sasaki, M., Li, X., Lin, B.M., Biskup, S., Zhang, L., Banerjee, R., Thomas, B., Yang, L. *et al.* (2009) Unexpected lack of hypersensitivity in LRRK2 knock-out mice to MPTP (1-methyl-4-phenyl-1,2,3,6-tetrahydropyridine). *J. Neurosci.*, **29**, 15846–15850.
33. Lee, M.K., Stirling, W., Xu, Y., Xu, X., Qui, D., Mandir, A.S., Dawson, T.M., Copeland, N.G., Jenkins, N.A. and Price, D.L. (2002) Human alpha-synuclein-harboring familial Parkinson's disease-linked Ala-53->Thr mutation causes neurodegenerative disease with alpha-synuclein aggregation in transgenic mice. *Proc. Natl Acad. Sci. USA*, **99**, 8968–8973.
34. von Coelln, R., Thomas, B., Andrabi, S.A., Lim, K.L., Savitt, J.M., Saffary, R., Stirling, W., Bruno, K., Hess, E.J., Lee, M.K. *et al.* (2006) Inclusion body formation and neurodegeneration are parkin independent in a mouse model of alpha-synucleinopathy. *J. Neurosci.*, **26**, 3685–3696.
35. Martin, L.J., Pan, Y., Price, A.C., Sterling, W., Copeland, N.G., Jenkins, N.A., Price, D.L. and Lee, M.K. (2006) Parkinson's disease alpha-synuclein transgenic mice develop neuronal mitochondrial degeneration and cell death. *J. Neurosci.*, **26**, 41–50.

36. Biskup, S., Moore, D.J., Celsi, F., Higashi, S., West, A.B., Andrabi, S.A., Kurkinen, K., Yu, S.W., Savitt, J.M., Waldvogel, H.J. *et al.* (2006) Localization of LRRK2 to membranous and vesicular structures in mammalian brain. *Ann. Neurol.*, **60**, 557–569.

37. Higashi, S., Moore, D.J., Colebrooke, R.E., Biskup, S., Dawson, V.L., Arai, H., Dawson, T.M. and Emson, P.C. (2007) Expression and localization of Parkinson's disease-associated leucine-rich repeat kinase 2 in the mouse brain. *J. Neurochem.*, **100**, 368–381.

38. Galter, D., Westerlund, M., Carmine, A., Lindqvist, E., Sydow, O. and Olson, L. (2006) LRRK2 expression linked to dopamine-innervated areas. *Ann. Neurol.*, **59**, 714–719.

39. Simon-Sanchez, J., Herranz-Perez, V., Olucha-Bordonau, F. and Perez-Tur, J. (2006) LRRK2 is expressed in areas affected by Parkinson's disease in the adult mouse brain. *Eur. J. Neurosci.*, **23**, 659–666.

40. Taymans, J.M., Van den Haute, C. and Baekelandt, V. (2006) Distribution of PINK1 and LRRK2 in rat and mouse brain. *J. Neurochem.*, **98**, 951–961.

41. Daher, J.P., Ying, M., Banerjee, R., McDonald, R.S., Hahn, M.D., Yang, L., Flint Beal, M., Thomas, B., Dawson, V.L., Dawson, T.M. *et al.* (2009) Conditional transgenic mice expressing C-terminally truncated human alpha-synuclein (alphaSyn119) exhibit reduced striatal dopamine without loss of nigrostriatal pathway dopaminergic neurons. *Mol. Neurodegener.*, **4**, 34.

42. West, M.J. (1993) New stereological methods for counting neurons. *Neurobiol. Aging.*, **14**, 275–285.

43. Pletnikova, O., West, N., Lee, M.K., Rudow, G.L., Skolasky, R.L., Dawson, T.M., Marsh, L. and Troncoso, J.C. (2005) Abeta deposition is associated with enhanced cortical alpha-synuclein lesions in Lewy body diseases. *Neurobiol. Aging*, **26**, 1183–1192.

44. Westerlund, M., Ran, C., Borgkvist, A., Sterky, F.H., Lindqvist, E., Lundstromer, K., Pernold, K., Brene, S., Kallunki, P., Fisone, G. *et al.* (2008) Lrrk2 and alpha-synuclein are co-regulated in rodent striatum. *Mol. Cell. Neurosci.*, **39**, 586–591.